Journal of
Applied Crystallography
ISSN 0021-8898

Received 29 April 2003
Accepted 23 October 2003

Quantitative microstructural and texture characterization by X-ray diffraction of polycrystalline ferroelectric thin films

Jesús Ricote[a]* and Daniel Chateigner[b]

[a]Instituto de Ciencia de Materiales de Madrid, CSIC, Cantoblanco, E-28049 Madrid, Spain, and [b]Laboratoire de Cristallographie et Sciences des Matériaux - ENSICAEN, F-14050 Caen, France. Correspondence e-mail: jricote@icmm.csic.es

Texture becomes an important issue in ferroelectric materials as it greatly influences the physical properties of polycrystalline films. The use of advanced methods of analysis of the X-ray diffraction profiles, namely quantitative texture analysis or the recently developed combined approach, allows access to quantitative information on the different components of the global texture and to more accurate values of structural and microstructural parameters of both the ferroelectric film and the substrate, not available by more conventional methods of analysis. The results obtained allow important conclusions to be drawn regarding the mechanisms that lead to the development of preferred orientations in thin films and, also, the correlation between them and the ferroelectric behaviour. For example, it is observed that the inducement of a strong ⟨111⟩ texture component does not mean the complete disappearance of the so-called 'natural' ⟨100⟩, ⟨001⟩ components, and that the ratio between the contributions to the global texture of these two components can be changed by the presence of tensile or compressive stress during crystallization of the films. The relative contributions of these texture components are also related to the final properties of the ferroelectric films.

1. Introduction

Ferroelectric materials, and specifically ferroelectric thin films, have attracted a great deal of attention recently due to their excellent polarization, dielectric, piezoelectric, pyroelectric and optical properties, used in a wide range of technological applications, from ferroelectric random access memories (FeRAM) (Scott, 2000) to microelectromechanical systems (Polla & Francis, 1996). X-ray diffraction has been routinely used as a non-destructive method of characterization of crystallographic structures, crystal size, strain state and texture of thin films. However, ferroelectric thin films present some specific problems that require the use of more advanced methods of X-ray analysis, in particular regarding texture.

Traditional methods of texture analysis produce coefficients indicating the degree of orientation of the polycrystal based on the analysis of the integrated intensities of the main X-ray reflections (Harris, 1952; Lotgering, 1959). The measurement of rocking curves has been used recently in the texture analysis of ferroelectric thin films (Legrand *et al.*, 1999). However, the only way to obtain quantitative information on the texture of the material is the measurement of pole figures and calculation of the orientation distribution function (Bunge, 1982): the so-called quantitative texture analysis. The function obtained contains information about all the components contributing to the texture and allows us to quantify the degree of orientation. In spite of the interest in this subject, complete quantitative studies of the pole figures are rarely found in the literature on ferroelectric thin films (Chateigner *et al.*, 1998; Ricote *et al.*, 2000).

A second important issue is that related to the application of classical diffraction approaches to anisotropic polycrystalline samples such as the ferroelectric thin films, which may be problematic. For example, a usual Bragg–Brentano diffraction diagram of a strongly textured film may not reveal all possible diffraction reflections, making structural determination impossible, which in turn prevents any quantitative texture analysis. This problem can be overcome by the relatively recently developed combined approach (Wenk *et al.*, 1994), which has proved to be a viable tool (Matthies *et al.*, 1997) and has been successfully applied to ferroelectric thin films (Cont *et al.*, 2002; Morales *et al.*, 2002).

In this work, we present the results obtained during the X-ray characterization of several ferroelectric thin films using the advanced techniques of analysis mentioned above: quantitative texture analysis and the combined approach. Some of the information obtained is not available by other more conventional methods of analysis. The results show the importance of the use of these methods, as they allows us to shed light on the mechanisms that lead to the development of preferred orientations in thin films and on their correlation with the ferroelectric behaviour.

2. X-ray diffraction characterization

Experimental pole figures were obtained using a Huber four-circle goniometer mounted on an X-ray generator. A $5^\circ \times 5^\circ$ grid measurement was carried out to cover the whole pole figure. A position-sensitive detector (INEL CPS-120), covering an angle of 120°, is used (spatial resolution 0.03°). The use of this kind of detector accelerates considerably the data acquisition compared with punctual detectors, but results in non-Bragg–Brentano or asymmetrical positions, which requires the localization of the peaks into the pole-figure coordinates as they do not correspond exactly to the goniometer rotation angles (Heizmann & Laruelle, 1986). Other effects, like the variations produced by changes in the probe volume and absorption in thin films, due to the fact that their thicknesses are less than the penetration depths, are also taken into account (Chateigner *et al.*, 1994). Pole-figure data are normalized into distribution densities and expressed as multiple of a random distribution (m.r.d.), which is equivalent to volume percentage per 1% area.

From the experimental pole figures we obtain the orientation distribution (OD) of the sample, $f(\mathbf{g})$, with $\mathbf{g} = \alpha\beta\gamma$, Euler angles. Only those pole figures that contain reliable information are used, after having checked that the data are sufficient to refine the full orientation distribution space. From the several methods of resolution of the OD we chose the WIMV (Williams–Imhof–Matthies–Vinel) iterative method (Matthies & Vinel, 1982), or the entropy-modified WIMV (E-WIMV) method (Liu *et al.*, 1993). The quality of the refinement is assessed by the reliability factors (RP0 and RP1, for global values and values above 1 m.r.d., respectively). From the OD we can determine the texture index $\{F^2 = (1/8\pi^2)\sum_i [f(g_i)]^2 \Delta g_i\}$, which is an indication of the degree of orientation of the material. Texture components are deduced from the calculated inverse pole figures, where we fix a sample direction and represent the distribution of the associated crystal directions. Calculations have been carried out with the *Berkeley Texture Package* (*BEARTEX*) (Wenk *et al.*, 1998).

An alternative method of analysis of the X-ray diffraction data, the so-called combined approach (Wenk *et al.*, 1994), has also been used. Briefly, the quantitative texture analysis is introduced into the Rietveld method, with the advantage that it can be easily combined with other analyses to mutual benefit, and, therefore, to allow a simultaneous and more precise determination of microstructural and structural parameters. Calculations were carried out with the *Materials Analysis Using Diffraction* package (MAUD) (Lutterotti *et al.*, 1999), in which the layered method (Tizliouine *et al.*, 1994) was implemented. This allows the analysis not only of the reflections coming from the ferroelectric thin film, but also from the Pt layer beneath.

3. Quantitative texture analysis of ferroelectric thin films

The ferroelectric thin films studied in this paper were obtained by deposition of sol–gel processed solutions, as reported elsewhere (Sirera & Calzada, 1995; Calzada *et al.*, 1998). Two compositions were used: $Pb_{0.76}Ca_{0.24}TiO_3$ (PTCa) and $Pb_{0.88}La_{0.08}TiO_3$ (PTL). In both cases the structure is tetragonal at room temperature, as corresponds to their Ca^{2+} (Chandra & Pandey, 2003) and La^{3+} (Hennings, 1971) contents, respectively. Solutions were spin-coated at 2000 r.p.m. for 45 s in a class 100 clean room. The wet films were partially pyrolized on a hot plate at 623 K for 60 s. Films of the required thickness were obtained by multiple-coating deposition on various platinized substrates in order to induce different textures. Crystallization was carried out typically by rapid thermal processing (RTP) (heating rate of 30 K s^{-1}) at 923 K for 50 s. The introduction of quantitative texture analysis as part of the characterization of these films allows us to obtain for the first time precise information on the efficiency of the different approaches used to obtain highly textured materials. This is shown in the following examples. We will refer mainly to the growth of films on substrates with unrelated structures, which results in axial symmetry, *i.e.* fibre textures, which can only be analysed by the study of complete pole figures, as in this work.

The simplest approach to produce different textured films is the modification of the substrate on top of which the film is deposited. Fig. 1 shows the different texture components obtained when an extra Ti layer is introduced on top of the original substrate. Although previous works had observed the inducement of the ⟨111⟩ texture component perpendicular to the film surface for lead-titanate-based thin films deposited on Ti layers (Muralt *et al.*, 1998; Calzada *et al.*, 2001), none of them was able to clarify whether this orientation, although dominant, is the only one occurring. From the inverse pole figures, not only can we observe texture components along the ⟨001⟩ and ⟨100⟩ directions, but we can also estimate their relative contribution. This leads us to conclude that, although the nucleation and growth of crystals oriented along ⟨111⟩ is strongly promoted, the so-called 'natural' orientation of these perovskites, along ⟨001⟩ and ⟨100⟩, is still present, each making a contribution to the global texture of 10–15%. In order to reduce such a contribution, it has been shown that it is possible to disrupt this 'natural' orientation process by annealing the substrate. This increases considerably the roughness of the Pt layer on top of which the film grows, resulting in an almost pure ⟨111⟩ orientation (Ricote, Morales & Calzada, 2002).

The polar axis in these compositions is along ⟨001⟩. Therefore, we are interested in a film with a preferred orientation along this direction. The problem is that this orientation is always associated with another orientation along ⟨100⟩, *i.e.* with the polar axis in the plane of the film, and, therefore, not contributing to the net polarization along the normal to the film surface. This is due to the fact that nucleation of oriented crystals takes place in the high-temperature cubic phase, where the two directions are equivalent. Nevertheless, the presence of tensile or compressive stress during the cooling process can favour one of the two directions (Ricote, Chateigner *et al.*, 2002). Among the possible origins of stress in films, we can make use of the different thermal expansion coefficients of the film and the substrate. The results obtained

by the use of different substrates are shown in Fig. 2. While the use of an Si-based substrate [$Pt/TiO_2/Si(100)$] produces a low-textured PTC–Si film, the choice of MgO(100) or $SrTiO_3$(100) instead of Si produces a stronger contribution of the ⟨001⟩ texture component, as shown by the larger density values in the centre of the corresponding pole figure. This is a consequence of the compressive stress developed in these films. The separation of these two texture components is difficult, as there is an important overlap of their corresponding diffraction peaks, which is not possible to study with the conventional methods of analysis.

The quantitative information on the texture of the films can be used to reveal tendencies that shed light on the mechanisms involved in the development of preferred orientations. This is clearly shown in the study of PTL films with varying thickness (Ricote, Poyato *et al.*, 2003). An increased number of deposited layers results in thicker films. Traditionally, the whole stack of deposited layers is crystallized in one step by direct insertion in a furnace. As we increase the number of layers we observe a decrease of the degree of orientation, *i.e.* the texture index. As this means a limitation of the film thickness to obtain highly textured films, we modify the crystallization by the so-called layer-by-layer process. This consists of the rapid thermal processing of each deposited layer before the following one is deposited. The results are shown in Fig. 3. Variations of the texture index by a maximum of 10% are obtained in this case, suppressing the thickness dependence of texture. In both cases we obtained a mixed ⟨100⟩, ⟨001⟩ orientation. No significant variations of the contributions of the texture components are observed. We conclude that the relative amount of crystals nucleated at the substrate–film interface with preferred orientation decreases as the film thickness increases. The layer-by-layer crystallization makes possible this kind of nucleation for each layer (this time on the layer-to-layer interface), and as a consequence the relative amount of oriented crystals remains almost constant as thickness increases. Of course, this is only valid if the nucleation of oriented crystals takes place on an interface. In the case of ⟨111⟩ orientations induced by the introduction of an extra Ti layer on the substrate (Fig. 4), the texture index decreases with an increasing number of deposited layers. This is due to the fact that, in this case, nucleation of ⟨111⟩-oriented crystals occurs only on the Ti layer. Therefore, the relative amount of these crystals decreases with increasing thickness of the film. This is also clear looking at the values of the ⟨111⟩ contribution to the texture, also plotted in Fig. 4. It can be seen that when the contribution of the ⟨111⟩ component is below ∼50%, the texture of the film starts to be dominated by the

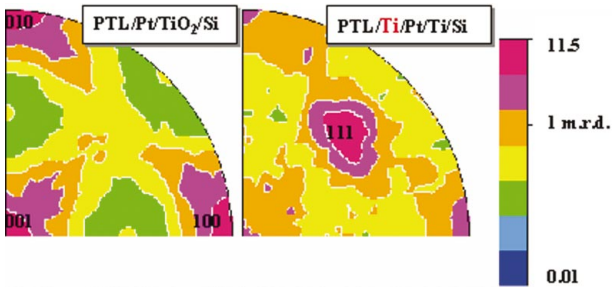

Figure 1
Inverse pole figures of PTL thin films showing the inducement of a strong ⟨111⟩ texture component by the introduction of an extra Ti layer on the substrate. Equal-area projection and logarithmic density scale.

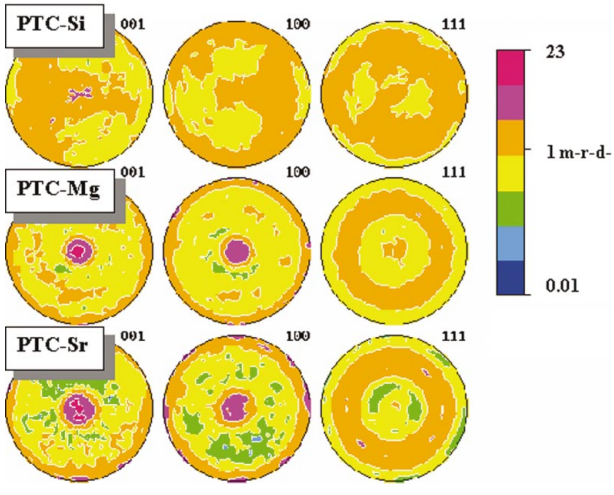

Figure 2
Recalculated pole figures for PTCa films deposited on different substrates: $Pt/TiO_2/Si$ (PTC-Si); Pt/MgO (PTC-Mg); $Pt/SrTiO_3$ (PTC-Sr). Equal-area projection and logarithmic density scale.

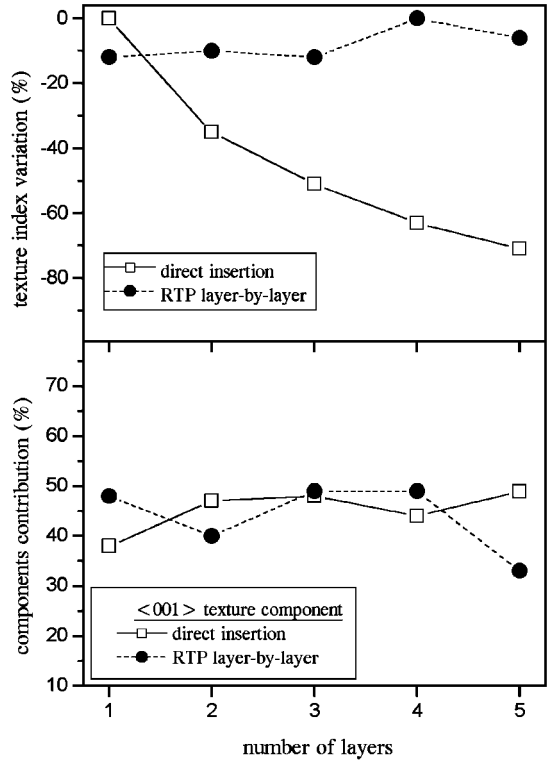

Figure 3
Evolution of the texture index and ⟨001⟩ texture component of PTL thin films with varying number of deposited layers. Two crystallization processes were used: direct insertion of the whole film in a furnace and a layer-by-layer rapid thermal processing (RTP). All films were deposited on $Pt/TiO_2/Si$.

Table 1
Correlation between the texture results and spontaneous pyroelectric coefficient (γ_s) for PTL thin films.

Texture components	F^2 (m.r.d.^{2})	γ_s (10^9 C cm^{-2} K^{-1})
⟨100⟩,⟨001⟩	4.6	4.8
	4.5	5.4
⟨111⟩	2.4	22.0
⟨100⟩,⟨001⟩	2.0	18.0

Table 2
Refined parameters for the PTCa and Pt layers using the combined approach (R_w = 7% and R_{Bragg} = 4.7%).

Layer	Thickness (Å)	F^2 (m.r.d.^{2})	RP0 (%)	Lattice parameters (Å)	μstrain
PTCa	4080 (1)	2	11	a = 3.945 (1), c = 4.080 (1)	0.0067 (1)
Pt	458 (3)	41	14	a = 3.955 (1)	0.0032 (1)

⟨001⟩ and ⟨100⟩ components. This means that the thickness effect on the texture disappears and the value of the texture index reaches a stable value.

The quantification of the texture of the films is also used to establish correlations with the physical properties, in particular those directly related to the polarization (Poyato *et al.*, 2001). An example is shown in Table 1. We clearly see the improvement of the spontaneous pyroelectric coefficient by the inducement of a ⟨111⟩ texture component. It must be remembered that crystals oriented along ⟨100⟩ directions (always associated with those oriented along ⟨001⟩) have the polar axis in the plane of the film and, therefore, do not contribute to the net polarization of the film. This negative effect on the final properties is not present in ⟨111⟩-oriented crystals. As a consequence we obtain improved pyroelectricity on films with this kind of texture component, as our results show. It is also possible to deduce other properties of the film (elastic, dielectric, piezoelectric) by obtaining a volume average of the tensor properties of the corresponding single crystal, taking into account the orientation distribution function (Ricote, Algueró & Chateigner, 2003).

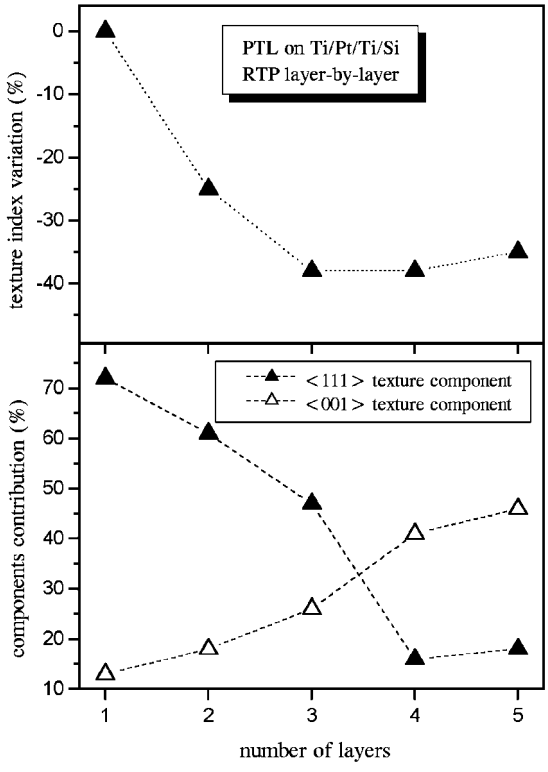

Figure 4
Evolution of the texture index and texture components of PTL thin films with varying number of deposited layers deposited on Ti/Pt/Ti/Si to induce ⟨111⟩ preferred orientation. A layer-by-layer rapid thermal processing (RTP) was used for all films.

4. Microstructural and structural characterization

The application of the combined approach to the characterization of ferroelectric thin films allows us to obtain simultaneously reliable information on texture, structure and microstructure of both the ferroelectric film itself and the Pt layer beneath. Up to now, X-ray diffraction was used either to obtain information on the phases present in the thin film or on its texture, normally using independent methods. Furthermore, reflections coming from any of the elements of the substrate were ignored. The main advance achieved with the combined analysis is that we obtain all the results contained in Table 2 with only one analysis. In addition, the results are more reliable. One of the main problems in the texture analysis of lead-titanate-based films on Pt-covered substrates is the overlap between peaks of reflections coming from the Pt and from the ferroelectric. This is solved with the combined approach. We extract results from the strong ⟨111⟩ orientation of the Pt and from the weak ⟨100⟩, ⟨001⟩ texture of the PTCa film. These are the expected results in both cases. The RP0 values in both cases are rather low, indicating a good refinement and the ability of the E-WIMV algorithm to represent both strong and weak textures simultaneously.

Refined thickness values of the two layers are very close to the calculated values for the deposition in the case of Pt (50 nm) and the values for the PTCa film measured by profilometry (∼400 nm). The lattice parameter obtained for the Pt is very similar to the value reported by Swanson (1953), a = 3.9231 Å. The only structural values available for the composition of the film studied here were provided by Mendiola *et al.* (1989). The reported values are a = 3.8939 Å and c = 4.0496 Å. Although structural distortions may be present in the polycrystalline thin films, the refined values are not close to the expected ones. One possible explanation may be the importance of the stress state in these films, which makes it necessary to introduce residual-stress determination in the combined analysis. This implementation is now available and has been used for layered structures (Lutterotti *et al.*, 2002); its application to ferroelectric thin films will be the focus of further work.

5. Final remark

In this paper, we have presented the progress in the field of ferroelectric thin films by the application of advanced X-ray diffraction techniques. As these techniques are still evolving, new, improved and more reliable results are expected in the near future that will allow us to solve further problems in the characterization by X-rays of these complex structures.

The authors wish to thank Dr M. L. Calzada, Dr M. Algueró and Ms R. Poyato for the preparation of the thin films studied in this work, and Dr L. Lutterotti and Mr L. Cont for their assistance in the application of the combined approach. X-ray measurements were carried out at the Laboratoire de Physique de l'État Condensé, Université du Maine - Le Mans (France). This work has been funded by the EU GROWTH project (G6RD-CT99-00169).

References

Bunge, H. J. (1982). *Texture Analysis in Materials Science.* London: Butterworths.

Calzada, M. L., Algueró, M. & Pardo, L. (1998). *J. Sol-Gel Sci. Technol.* **13**, 837–841.

Calzada, M. L., Poyato, R., García López, J., Respaldiza, M. A., Ricote, J. & Pardo, L. (2001). *J. Eur. Ceram. Soc.* **21**, 1529–1533.

Chandra, A. & Pandey, D. (2003). *J. Mater. Res.* **18**, 407–414.

Chateigner, D., Germi, P. & Pernet, M. (1994). *Mater. Sci. Forum*, **157–162**, 1379–1386.

Chateigner, D., Wenk, H. R., Patel, A., Todd, M. & Barber, D. J. (1998). *Integrated Ferroelect.* **19**, 121–140.

Cont, L., Chateigner, D., Lutterotti, L., Ricote, J., Calzada, M. L. & Mendiola, J. (2002). *Ferroelectrics*, **267**, 323–328.

Harris, G. B. (1952). *Philos. Mag.* **43**, 113–123.

Heizmann, J. J. & Laruelle, C. (1986). *J. Appl. Cryst.* **19**, 467–472.

Hennings, D. (1971). *Mater. Res. Bull.* **6**, 329–340.

Legrand, C., Yi, J. H., Thomas, P., Guinebretiére, R. & Mercurio, J. P. (1999). *J. Eur. Ceram. Soc.* **19**, 1379–1381.

Liu, Y., Wang, F., Xu, J. & Liang, Z. (1993). *J. Appl. Cryst.* **26**, 268–271.

Lotgering, F. K. (1959). *J. Inorg. Nucl. Chem.* **9**, 113–123.

Lutterotti, L., Matthies, S., Chateigner, D., Ferrari, S. & Ricote, J. (2002). *Mater. Sci. Forum*, **408–412**, 1603–1608.

Lutterotti, L., Matthies, S. & Wenk, H. R. (1999). *Proceedings of the 20th International Conference on Textures of Materials*, Vol. 2, edited by J. A. Szpunar, pp. 1599–1604. Montreal: NRC Research Press.

Matthies, S., Lutterotti, L. & Wenk H. R. (1997). *J. Appl. Cryst.* **30**, 31–42.

Matthies, S. & Vinel, G. W. (1982). *Phys. Status Solidi B*, **112**, K111–K120.

Mendiola, J., Jiménez, B., Alemany, C., Pardo, L. & Del Olmo, L. (1989). *Ferroelectrics*, **94**, 183–188. (JCPDS file 39-1336.)

Morales, M., Chateigner, D., Lutterotti, L. & Ricote, J. (2002). *Mater. Sci. Forum*, **408–412**, 113–118.

Muralt, P., Maeder, T., Sagalowicz, L., Hiboux, S., Scalese, S., Naumovic, D., Agostino, R. G., Xanthopoulos, N., Mathieu, H. J., Patthey, L. & Bullock, E. L. (1998). *J. Appl. Phys.* **83**, 3835–3841.

Polla, D. L. & Francis, L. F. (1996). *MRS Bull.* **21**, 59–65.

Poyato, R., Calzada, M. L., Ricote, J., Pardo, L. & Willing, B. (2001). *Integrated Ferroelectr.* **35**, 77–86.

Ricote, J., Algueró, M. & Chateigner, D. (2003). *Mater. Sci. Forum*, **426–432**, 3433–3438.

Ricote, J., Chateigner, D., Calzada, M. L. & Mendiola, J. (2002). *Bol. Soc. Esp. Cerám. Vidrio.* **41**, 80–84.

Ricote, J., Chateigner, D., Pardo, L., Algueró, M., Mendiola, J. & Calzada, M. L. (2000). *Ferroelectrics*, **241**, 167–174.

Ricote, J., Morales, M. & Calzada, M. L. (2002). *Mater. Sci. Forum*, **408–412**, 1543–1548.

Ricote, J., Poyato, R., Algueró, M., Pardo, L., Calzada, M. L. & Chateigner, D. (2003). *J. Am. Ceram. Soc.* **86**, 1571–1577.

Scott, J. F. (2000). *Ferroelectric Memories. Springer Series in Advanced Microelectronics 3*. Berlin-Heidelberg: Springer-Verlag.

Sirera, R. & Calzada, M. L. (1995). *Mater. Res. Bull.* **30**, 11–18.

Swanson, T. (1953). *Natl Bur. Stand. (US)*, Circ. 539, I, 31. (JCPDS file 04-0802.)

Tizliouine, A., BessièRes, J., Heizmann, J. J. & Bobo, J. F. (1994). *Mater. Sci. Forum*, **157**, 227–234.

Wenk, H. R., Matthies, S., Donovan, J. & Chateigner, D. (1998). *J. Appl. Cryst.* **31**, 262–269.

Wenk, H. R., Matthies, S. & Lutterotti, L. (1994). *Mater. Sci. Forum*, **157–162**, 473–479.